PHYSICAL REVIEW B **92**, 220418(R) (2015)

# Mechanism for nuclear and electron spin excitation by radio frequency current

Stefan Müllegger,[1,*] Eva Rauls,[2,†] Uwe Gerstmann,[2] Stefano Tebi,[1] Giulia Serrano,[1] Stefan Wiespointner-Baumgarthuber,[1] Wolf Gero Schmidt,[2] and Reinhold Koch[1]

[1]*Institute of Semiconductor and Solid State Physics, Johannes Kepler University Linz, 4040 Linz, Austria*

[2]*Lehrstuhl für Theoretische Physik, University of Paderborn, 33098 Paderborn, Germany*

(Received 8 October 2015; revised manuscript received 30 November 2015; published 23 December 2015)

Recent radio frequency scanning tunneling spectroscopy (rf-STS) experiments have demonstrated nuclear and electron spin excitations up to $\pm 12\hbar$ in a single molecular spin quantum dot (qudot). Despite the profound experimental evidence, the observed independence of the well-established dipole selection rules is not described by existing theory of magnetic resonance—pointing to a new excitation mechanism. Here we solve the puzzle of the underlying mechanism by discussing the relevant mechanistic steps. At the heart of the mechanism, periodic transient charging and electric polarization due to the rf-modulated tunneling process cause a periodic asymmetric deformation of the adsorbed qudot, enabling efficient spin transitions via spin-phonon-like coupling. The mechanism has general relevance for a broad variety of different spin qudots exhibiting internal mechanical degrees of freedom (organic molecules, doped semiconductor qudots, nanocrystals, etc.).

DOI: 10.1103/PhysRevB.92.220418 PACS number(s): 75.50.Xx, 68.37.Ef, 73.50.Rb, 75.78.−n

Recently, we introduced the technique of radio frequency scanning tunneling spectroscopy (rf-STS) [1] by investigating a molecular spin quantum dot (qudot), namely, a single molecule of the archetypal terbium double-decker ($TbPc_2$) [2] single-ion magnet on a Au(111) substrate. By utilizing resonant rf current, we succeeded in demonstrating excitation of electron and nuclear spin transitions in these qudots. The observed changes of electron ($J$) and nuclear ($I$) angular momentum components of up to $\Delta J_z = \pm 12$ or nuclear $\Delta I_z = \pm 3$ [1] contradict the electromagnetic dipole selection rules ($\Delta J_z = \pm 1$ and $\Delta I_z = \pm 1$), which govern the well-established methods of electron and nuclear magnetic resonance. This points towards a novel spin-excitation channel by rf-STS, which is fundamentally different from photon-induced spin-excitation processes driven by electromagnetic dipole transitions. Our rf-STS experiments [1,3] revealed that electron tunneling via molecular orbitals (MOs) of $TbPc_2$ is crucial for rf-STS-based spin excitation. The necessity of orbital-mediated electron tunneling in rf-STS is in marked contrast to spin excitation by inelastic dc electron tunneling [4–6]; the latter occurs at characteristic threshold energies symmetrically above and below the Fermi energy ($E_F$); higher spin excitations are sequential two- or three-step processes with $\Delta J_z = \pm 1$ for each step [6]. Most of the observed high spin excitations are far away from so-called avoided level crossings [1], ruling out a dominant role of quantum tunneling of magnetization. The intriguing evidence for efficient higher spin excitations via one-step excitation processes in rf-STS points towards the involvement of mechanical degrees of freedom [3] for fulfilling the fundamental angular momentum conservation [7].

In this Rapid Communication, we present a mechanism that explains spin excitations by rf-STS in a single molecular spin qudot. The mechanism is confirmed by first-principles calculations using density functional theory (DFT), which show that the internal mechanical degrees of freedom of a molecular spin qudot play a crucial role for spin excitation in an rf-STS experiment. At the heart of the mechanism lie the periodic transient charging and electric polarization of the qudot due to the rf-modulated tunneling process. The rf modulation induces periodic electronic and structural perturbations in the qudot—absent in stochastic dc-STM experiments. The resulting mechanical oscillations enable angular momentum transfer between the qudot's spin and its mechanical backbone, similar to the role of phonons in spin-phonon coupling. By lowering the symmetry and by increasing the qudot's internal strain, the presence of the substrate makes the mechanism very efficient.

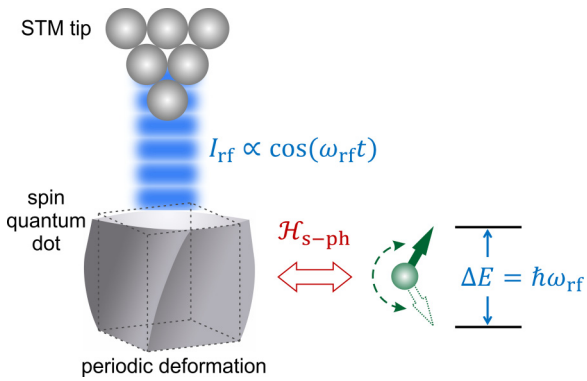


FIG. 1. (Color online) Schematic illustration of resonantly exciting a spin transition in a molecular spin qudot in an rf-STS experiment by mechanical deformation due to rf-modulated tunneling current $I_{rf}$.

In the following we show that in an rf-STS experiment (Fig. 1), the qudot's mechanical structure is periodically deformed by the rf-modulated electron tunneling process at frequency $\omega_{rf}$ [3]. The modulation adds a periodic component to the initially random tunneling of electrons. Based on the experimental results of Ref. [1], a comprehensive description of the rf-STS mechanism has to take into account the transient electric charging of the qudot by the STM tip as well as substrate effects. Besides charging, already the presence of the electric ($E$) field of the STM tip can affect the mechanical

*Corresponding author: stefan.muellegger@jku.at
†Corresponding author: eva.rauls@upb.de

 

structure of the molecule during an rf-STS experiment. To investigate details of the mechanism by theoretical modeling, the simulation of a model system as realistic as possible, i.e., including a proper description of the substrate, is mandatory. Herein, the model system is represented by single $TbPc_2$ molecules on Au(111), as studied in Ref. [1]. Isolated $TbPc_2$ in the gas phase consists of a $Tb^{3+}$ ion with total electronic angular momentum of $J = 6$ and nuclear spin $I = 3/2$ sandwiched between two organic phthalocyanine (Pc) ligands [2]. The ligand field stabilizes a strong uniaxial magnetic anisotropy with a ground-state doublet $J_z = \pm 6$ [8]. This doublet is coupled by the additional transverse magnetic anisotropy of the ligand field, relaxing the selection rules for spin-phonon coupling $\Delta J_z = \pm 1$ (for $m_s \approx 0$) and $\Delta J_z = \pm 2$ (for large $m_s \approx \pm S$) that follow from the spin-phonon Hamiltonian [9]:

$$\mathcal{H}_{\text{s-ph}} = \sum_{\alpha,\beta,\mu,\nu} \Lambda_{\alpha\beta}^{\mu\nu} \frac{\partial u_\alpha}{\partial r_\beta} S_\mu S_\nu. \quad (1)$$

Our DFT results reveal that the presence of the substrate increases the transverse local strain $e_{\alpha\beta} = \frac{\partial u_\alpha}{\partial r_\beta}$ $(\alpha, \beta = x, y)$ by about one order of magnitude, further relaxing the selection rules and considerably enhancing the transition probabilities for higher spin flips. Based on elasticity theory, we estimate that a change of the qudot's mechanical angular momentum of $12\hbar$ within 1 ns exerts a torque causing mechanical shear deformation of $<10$ fm (assuming a $1 \times 1 \times 0.4$ nm$^3$ qudot with $\approx 5$ GPa shear elastic modulus typical of phthalocyanine molecular films [10]).

As shown in Ref. [1], the observation of an rf-STS signal relies on electron flow through an MO of the molecular qudot. Each tunneling electron transiently charges the molecular qudot. If the electron lifetime in the MO (before leaving to the substrate) $\tau_{\text{MO}}$ is sufficiently long, the transient electron polarizes the qudot, slightly altering atom positions and bond lengths within the dot by partial de-/repopulation of MOs. The situation is similar to the temporary formation of a molecular polaron (i.e., deformation caused by electric polarization). For $TbPc_2$-based tiny qudots, the lowest (completely) unoccupied MO, utilized for rf-STS tunneling experiments in Ref. [1], is essentially a $\pi$ orbital of the Pc ligands [11]. From the lifetime of excited charge states in a Pc monolayer on metal surface a value of $\tau_{\text{MO}} \approx 10^{-9}$ s was estimated by Takagi *et al.* [12], which is a value similar to that of the bulk phase [13]. In contrast, the molecular backbone adopts its mechanical structure at a much shorter time scale of $10^{-12}$ s, assuring (quasi) equilibrium conditions for the charge-induced structural change. The transiently charged qudot adopts a ground-state configuration with a different mechanical structure compared to the neutral one [11]. This polarization-induced mechanical deformation is similar to the polaron-induced mechanical switching of single-molecule junctions discussed by Galperin *et al.* [14].

For $TbPc_2$/Au(111), we study herein the polaronlike effect upon transient charging with first-principles calculations. As discussed above, the inclusion of the substrate is essential, but makes time-dependent dynamic modeling numerically by far too expensive. For a quantitative determination of lifetimes, we expect spin-orbit coupling to play an important role. Nevertheless, reliable ground-state geometries and related

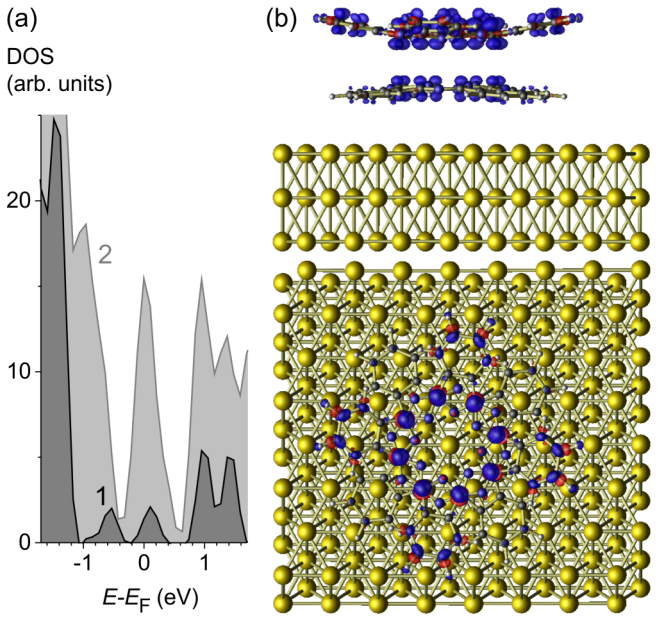


FIG. 2. (Color online) Neutral $[TbPc_2]^0$ molecule adsorbed on Au(111). (a) Calculated density of states (DOS), comparing the $TbPc_2$ part (curve 1) with the total DOS (curve 2). (b) Charge density plot of the partially occupied MOs at the Fermi energy in side view (top) and top view (bottom).

mechanical properties are obtained by a scalar-relativistic treatment, also for systems with exceptionally strong spin-orbit coupling [15,16]. Hence, for the quasiequilibrium conditions described above, we have performed static DFT calculations by (i) adding one extra electron to the neutral structure and (ii) applying an external electric field parallel to the substrate normal.

For the DFT calculations we employ the Vienna *ab initio* Simulation Package (VASP) [17] including a supercell approach and periodic boundary conditions for an accurate description of the electronic structure of the metallic Au(111) surface. The latter is crucial for a realistic occupation of the qudot's MOs: Figure 2(a) shows the density of states (DOS) of a neutral $TbPc_2$ adsorbed on Au(111). Notice that the state centered at $+0.1$ eV is partially ($\approx 40\%$) occupied, defining $E_{\text{F}}$ of the system. In contrast, the MO originating from the lowest unoccupied molecular orbital of the isolated molecule is found $\approx 1$ eV above $E_{\text{F}}$. We describe electron/ion interactions in scalar-relativistic approximation by the projector-augmented wave method [18] and the electron-electron exchange-correlation energy by the generalized gradient approximation [19]. The influence of dispersive interactions is included via the semiempirical London dispersion formula [20]. Following the experimental observation of $Tb^{3+}$-like spectra in Ref. [1], the $4f$ shell of the Tb ion is fixed in a trivalent configuration and treated as core electrons. We use an energy cutoff of 400 eV for the plane wave basis set and the $\Gamma$ point for the Brillouin zone modeling. The Au surface is modeled by three layers, the lowest kept fixed at bulk position during relaxation, while all other atoms are allowed to relax freely. A vacuum layer of 2.5 nm is found to be sufficient to avoid artificial interactions between periodic images parallel to the substrate normal

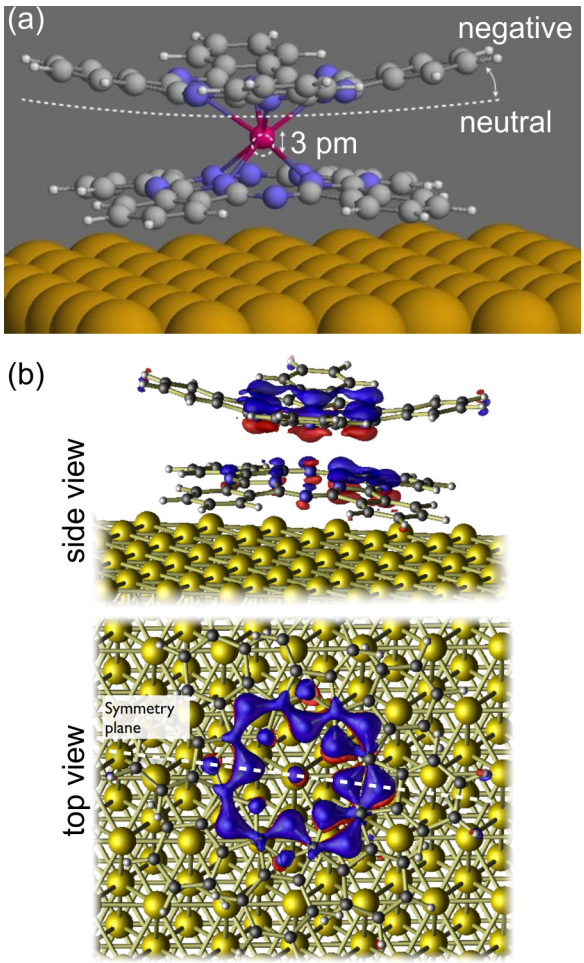


FIG. 3. (Color online) Negatively charged $[TbPc_2/Au(111)]^-$. (a) DFT structure; dotted white lines indicate the structure of the neutral $[TbPc_2/Au(111)]^0$ molecule. (b) Distribution of the extra electron in the charged state after full electronic and structural relaxation; blue (red) indicates electron accumulation (depletion).

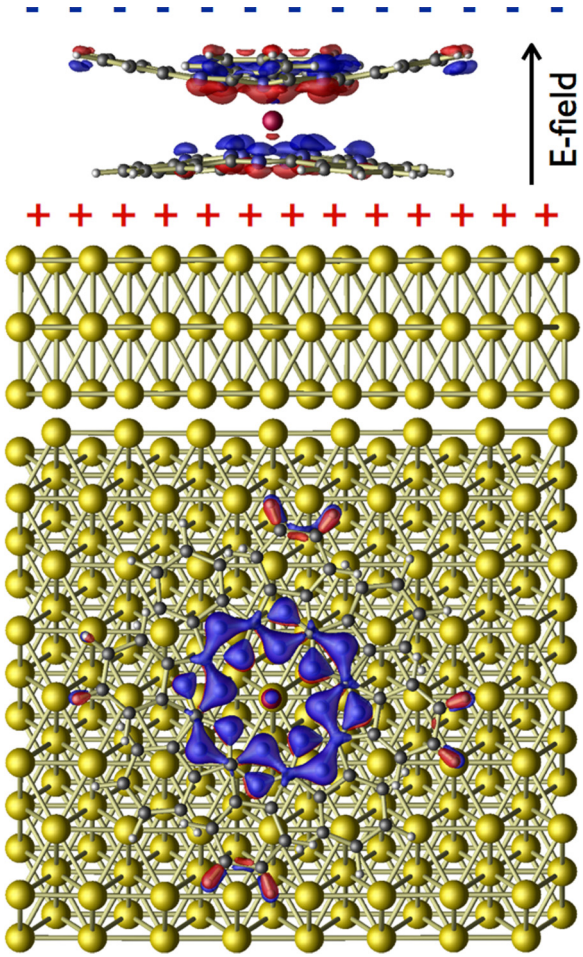


FIG. 4. (Color online) DFT relaxed structure of neutral $[TbPc_2]^0$ on Au(111) under the presence of an electric field of 5 V/nm perpendicular to the surface; blue (red) indicates electron accumulation (depletion).

($z$ axis), also allowing one to take into account the external $E$ field by adding a potential $E \cdot z$.

In a first step, as a starting model for the transient charging process, we add a permanent extra electron to the system, i.e., we investigate $[TbPc_2/Au(111)]^-$. The extra electron raises $E_F$ by about 0.14 eV, but leaves the spectral shape of the DOS almost unchanged. Figure 3(a) illustrates the resulting polaronic deformation. Compared to the neutral form (dotted lines), the $TbPc_2$ molecule in the negatively charged system exhibits a more strongly bent upper Pc ligand and increased vertical distance to the substrate surface. In particular, the $Tb^{3+}$ ion lies $\approx$3 pm farther away from the substrate. In this respect, our results are consistent with earlier gas phase calculations by Takamatsu and Ishikawa [11] reporting that neutral $[TbPc_2]^0$ has a 10 pm shorter Pc-Pc distance than $[TbPc_2]^-$ due to increased bond order by emptying an antibonding MO. To understand further details of the mechanism, the substrate and the STM tip play a crucial role. For the neutral structure $[TbPc_2/Au(111)]^0$ [Fig. 2(b)], the frontier MOs consist of a superposition of energetically degenerate orbitals, resulting in a symmetric charge distribution predominantly localized at the upper Pc ligand. Due to the substrate-induced metallic occupation of the MO close to $E_F$, very small noncentrosymmetric perturbations are sufficient to lift the degeneracy. This causes some structural relaxation as well as an asymmetric charge density, both further increasing the mechanical angular momentum of the system.

Figure 3(b) shows that after full structural relaxation, the induced charge distribution in $[TbPc_2/Au(111)]^-$ becomes inhomogeneous: asymmetric in charge and also slightly in structure (due to weak symmetry breaking by the substrate). The pyrrole groups of the upper molecule are no longer at the same height above the surface but differ by $\approx$2 pm, whereby the phtalocyanine ligand with the larger part of the induced density of the extra electron is stronger bent and lifted. Slightly smaller is the difference for the nitrogen atoms. It is reasonable to assume that this plot obtained for the negatively charged species actually represents a snapshot of the transient charging process just before the electron flows off to full extent to the substrate; remember, it stays about 1 ns in the molecule. It is also important to note here, that small external perturbations such as, e.g., a small off-center positioning of the STM tip are expected as further efficient driving forces to break the symmetry, as well.

The relaxation towards an asymmetric configuration may also be facilitated by the $E$ field due to the bias voltage between the sample and STM tip. To see that, it is illustrative to discuss the effect of the $E$ field separately, i.e., independent of the above-mentioned charging mechanism. Hence, onto the neutral system we have applied a homogeneous $E$ field [21] perpendicular to the substrate. Like in experiment, the system behaves critically with respect to the $E$-field strength: Visible effects are obtained in a range of 0.5–5 V/nm. Above 5 V/nm the $TbPc_2$ molecule starts to dissociate. This is in full agreement with our experimental $E$-field value of 4 V/nm causing dissociation of $TbPc_2$ molecules on Au(111).

Figure 4 shows that an $E$ field of 5 V/nm induces a structural relaxation of neutral $[TbPc_2/Au(111)]^0$ similar to that of the negatively charged system [Fig. 3(b)]. The Pc-Pc distance is increased by nearly 30 pm, whereby the Tb ion lies ≈16 pm farther away from the substrate. Again, the structural relaxation originates from a shift of the energy levels of the $TbPc_2$ molecule with respect to those of the substrate, resulting in a redistribution of electron density. Similar to a rigid charging, the presence of an $E$ field induces electron density into partially occupied antibonding MOs. This effect becomes also visible by the corresponding charge redistribution (Fig. 4) which strongly resembles that of the extra electron in the negatively charged system [Fig. 3(b)], in particular reflecting the same reduced symmetry.

Summarizing our results, the DFT simulations confirm that neutral and charged $TbPc_2$ molecules on Au(111) have different structures with different mechanical properties. Our findings reveal that the interactions of $TbPc_2$ with the substrate and/or the STM tip slightly lift the degeneracy of its frontier MOs. Such small perturbations are necessary and sufficient for an asymmetric density distribution of the antibonding MOs of the system. This asymmetry causes asymmetric mechanical deformation of the $TbPc_2$ molecule, giving rise to nonzero shear components in the respective strain tensor, crucial for the rf-STS mechanism, enabling high spin transitions, as observed in Ref. [1]. By this, our calculations provide a natural explanation for the rf-STS-induced spin excitation: From magnetic resonance on bulk samples it is well known that angular momentum may readily be transferred between spin and mechanical degrees of freedom, i.e., phonons. Spin-phonon effects play an important role, e.g., for conservation of angular momentum in the famous Barnett [22] and Einstein-de Haas effect [23]. Moreover, angular momentum transfer pathways have been experimentally observed between spins and thermal phonons [24], ultrasonic waves in magnetic molecules [25,26], and mechanical modes of nanoresonators [27,28]. In the present case, the periodic mechanical deformation of $TbPc_2$ is responsible for an additional (perturbative) component in the spin Hamiltonian. The latter depends on the (periodically in time modulated) positions of $TbPc_2$'s atoms, thus (i) establishing a coupling of mechanical with spin degrees of freedom and (ii) thereby coupling different spin states of the qudot. This mixing of states enables transitions between different spin states, such as periodically excited spin transitions at resonance, i.e., for $\omega_{\mathrm{rf}} = \Delta E_{\mathrm{spin}}/\hbar$ as reported in Ref. [1] (Fig. 1).

The spin excitation mechanism presented herein was introduced by means of spin qudots represented by single terbium (III) double-decker molecules, which exhibit a rich spectrum of mechanical degrees of freedom. We remark, however, that the presented mechanism for rf-induced spin excitation has a much more general relevance. It can be extended to a broad variety of different spin qudots exhibiting internal mechanical degrees of freedom (organic molecules, doped semiconductor qudots, nanocrystals, etc.). Furthermore, the proposed mechanism is not restricted to tunneling electrons but is also valid for other types of conductance.

We kindly acknowledge financial support of the project I958 by the Austrian Science Fund (FWF) and the Deutsche Forschungsgemeinschaft (DFG) as well as the DFG priority program SPP 1601.

[1] S. Müllegger, S. Tebi, A. K. Das, W. Schöfberger, F. Faschinger, and R. Koch, Phys. Rev. Lett. **113**, 133001 (2014).

[2] N. Ishikawa, M. Sugita, and W. Wernsdorfer, Angew. Chem., Int. Ed. **44**, 2931 (2005).

[3] S. Müllegger, A. K. Das, K. Mayr, and R. Koch, Nanotechnology **25**, 135705 (2014).

[4] A. J. Heinrich, J. A. Gupta, C. P. Lutz, and D. M. Eigler, Science **306**, 466 (2004).

[5] Y.-S. Fu, T. Zhang, S.-H. Ji, X. Chen, X.-C. Ma, J.-F. Jia, and Q.-K. Xue, Phys. Rev. Lett. **103**, 257202 (2009).

[6] S. Loth, M. Etzkorn, C. P. Lutz, D. M. Eigler, and A. J. Heinrich, Science **329**, 1628 (2010).

[7] D. A. Garanin and E. M. Chudnovsky, Phys. Rev. B **92**, 024421 (2015).

[8] S. Thiele, R. Vincent, M. Holzmann, S. Klyatskaya, M. Ruben, F. Balestro, and W. Wernsdorfer, Phys. Rev. Lett. **111**, 037203 (2013).

[9] D. Gatteschi, R. Sessoli, and J. Villain, *Molecular Nanomagnets* (Oxford University Press, Oxford, 2006).

[10] M. Kanari, H. Kawamata, and T. Wakamatsu, Appl. Phys. Lett. **90**, 061921 (2007).

[11] S. Takamatsu and N. Ishikawa, Polyhedron **26**, 1859 (2007).

[12] S. Takagi, T. Shimada, M. Eguchi, T. Yui, H. Yoshida, D. A. Tryk, and H. Inoue, Langmuir **18**, 2265 (2002).

[13] L. T. Ueno, C. C. Jayme, L. R. Silva, E. B. Pereira, S. M. de Oliveira, and A. E. H. Machado, J. Braz. Chem. Soc. **23**, 2237 (2012).

[14] M. Galperin, M. A. Ratner, and A. Nitzan, Nano Lett. **5**, 125 (2005).

[15] U. Gerstmann, N. J. Vollmers, A. Lücke, M. Babilon, and W. G. Schmidt, Phys. Rev. B **89**, 165431 (2014).

[16] C. Klein, N. J. Vollmers, U. Gerstmann, P. Zahl, D. Lükermann, G. Jnawali, H. Pfnür, C. Tegenkamp, P. Suter, W. G. Schmidt, and M. Horn-von Hoegen, Phys. Rev. B **91**, 195441 (2015).

[17] G. Kresse and J. Furthmueller, Comput. Mater. Sci. **6**, 15 (1996).

[18] G. Kresse and D. Joubert, Phys. Rev. B **59**, 1758 (1999).

[19] J. P. Perdew, J. A. Chevary, S. H. Vosko, K. A. Jackson, M. R. Pederson, D. J. Singh, and C. Fiolhais, Phys. Rev. B **46**, 6671 (1992).

[20] F. Ortmann, F. Bechstedt, and W. G. Schmidt, Phys. Rev. B **73**, 205101 (2006).
[21] G. Makov and M. C. Payne, Phys. Rev. B **51**, 4014 (1995).
[22] S. J. Barnett, Phys. Rev. **6**, 239 (1915).
[23] A. Einstein and W. J. De Haas, Verh. Dtsch. Phys. Ges. **17**, 152 (1915).
[24] K. S. Tikhonov, J. Sinova, and A. M. Finkel'stein, Nat. Commun. **4**, 1945 (2013).
[25] C. Calero, E. M. Chudnovsky, and D. A. Garanin, Phys. Rev. B **76**, 094419 (2007).
[26] C. Calero and E. M. Chudnovsky, Phys. Rev. Lett. **99**, 047201 (2007).
[27] D. A. Garanin and E. M. Chudnovsky, Phys. Rev. X **1**, 011005 (2011).
[28] E. M. Chudnovsky and D. A. Garanin, Phys. Rev. B **89**, 174420 (2014).